Melvin Satterwhite
U.S. Army Engineer Topographic Laboratories
Fort Belvoir, VA 22060
William Rice
Jerome Shipman
IBM Federal Systems Division
Gaithersburg, MD 20879

Using Landform and Vegetative Factors to Improve the Interpretation of Landsat Imagery

Land-cover units associated with major landform conditions were readily classified with reasonable accuracy to level 3 and at times to level 4.

INTRODUCTION

CLASSIFYING land cover and land use by applying pattern classification algorithms to digital multispectral sensor data has become increasingly common since the technique was first proposed (Fu

have been classified by this method for agricultural and forest inventories and geological prospecting. In particular, investigators have evaluated this use of multispectral scanner digital data in order to map and inventory forested and rangeland resources.

ABSTRACT: *A general classification of land use/land cover to level 2 can be obtained from Landsat data by using supervised digital classification techniques. However, because different land-cover classes often fall into the same spectral class, a finer level of detail cannot be readily achieved in the Landsat imagery. The purpose of this study was to evaluate digitally classified Landsat imagery and to determine those vegetative and terrain factors that could aid in the interpretation of the imagery. A methodology was developed for comparing descriptive landform and land-cover ground truth data with the corresponding digital imagery which exploited knowledge of (1) plant community and landform relations, (2) the species phenological and physiognomic characteristics, and (3) the reflectance-cover relationships.*

Using this methodology, land-cover units associated with major landform conditions were readily classified with reasonable accuracy to level 3 and at times to level 4. Where these levels of classification could not be achieved, the factors causing misclassification were determined. The most important factors were found to be (1) the composition and role of the species in the different land-cover units; (2) difference in vegetative cover, particularly in those land cover units with either a sparse or very dense cover; (3) the lack of characterizing spectral signatures from the dominant plant species; (4) the signature of the surface materials (gravel covered surfaces were often spectrally similar to the bedrock from which they were derived); and (5) the spatial and spectral resolution of the Landsat imagery.

et al., 1969). The most widely used algorithm is maximum likelihood classification based upon the assumption that the spectral signature vector is normally distributed (Fu, 1976). Many Landsat scenes

These resulting land-cover maps usually depict broad categories successfully classified to level 2 of Anderson's land-use/land-cover classification system (Anderson *et al.*, 1976). The spectral similarity of

some land-cover units and the image resolution have limited the differentiation of the level 2 classification.

The accuracy of a land-cover classification in an arid to semi-arid region is further limited by the narrow brightness range in the Landsat bands, and by the lack of discreteness in the signatures associated with the land-cover units and their plant and soil reflectance characteristics. Frequently, different plant communities have similar spectral signatures and are accordingly classified as the same spectral unit. It appears that, to resolve this confusion and to achieve a higher level of classification, an understanding of plant phenological characteristics and plant habit requirements should be incorporated into the digital image analysis and evaluation process.

OBJECTIVES

Previous field and laboratory studies have described the relation between land-cover and landform conditions for identifying terrain conditions using medium scale aerial photography (Satterwhite and Ehlen, 1980). Relations between cover, soil, and plant reflectance in the four Landsat bands are related to the percent cover of the soil-vegetation targets (Satterwhite *et al.*, 1982).

The principal objective of the present study is to apply the findings of the above studies, together with an understanding of the plant phenological characteristics, in order to develop a methodology to improve the classification of Landsat data. The improvement in classification accuracy will be quantified by determining the increase in the level of classification obtainable with the new methodology.

In those cases where classification accuracy cannot be improved using the new methodology, it is the second objective of the study to identify the factors causing misclassification and to determine whether they naturally limit obtainable classification accuracy or whether obtaining more data may be expected to be fruitful.

THE STUDY AREA

The area studied is in south central New Mexico and western Texas (Figure 1). This area is part of the Northern Chihuahuan Desert, previously studied by Satterwhite and Ehlen (1980) to determine its landforms and land-use/land-cover conditions. Dominate shrub communities in this area are *Prosopis glandulosa*, *Larrea tridentata*, *Flourensia cernua*, and *Artemisia filifolia*. Sizable grasslands are also found, consisting of *Bouteloua eriopoda*, *B. curtipendula*, *B. gracilis*, and *Sporobolus flexuosus*, but encroachment of the shrub species into these grasslands is evident.

The land-cover maps, from which Figure 2 was excerpted, were produced from an intensive field survey and mapping effort of the land-cover condi-

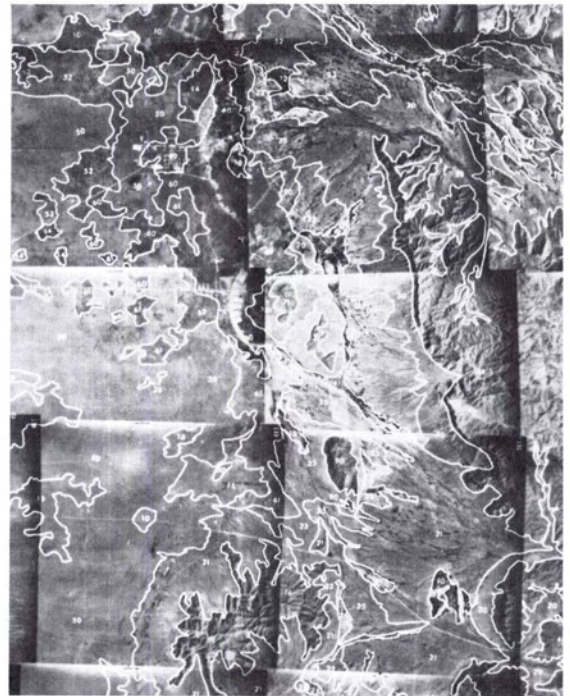FIG. 1.   Location map showing the Dona Ana and Meyer Study Areas.

FIG. 2.   Ground truth land-cover map for the Meyer study area (From Satterwhite and Ehlen, 1980)

tions during August-September 1977 and 1978. Table 1 provides the legend for Figure 2. Panchromatic aerial photography was used for mapping the plant communities (Satterwhite and Ehlen, 1980).

MATERIALS AND METHODS

The area was classified by a maximum likelihood algorithm, which maximizes the proportion of correctly assigned observations when the data can be represented by multivariate normal distributions. This algorithm is a supervised, parametric classification technique and requires a spectral signature composed of a mean vector ($\boldsymbol{\mu}_k$) and a covariance matrix ($\boldsymbol{\Sigma}_k$) for each class. According to this algorithm, an observation vector is classified into the class with the smallest value of

$$L_k(x) = \log|\Sigma_k| + (\mathbf{x} - \boldsymbol{\mu}_k)^{\mathrm{T}} \Sigma_k^{-1} (\mathbf{x} - \boldsymbol{\mu}_k) - 2 \log P_k \qquad (1)$$

where

$|\Sigma_k|$ = the determinant of the covariance matrix for the kth class,
$\boldsymbol{\mu}_k$ = the mean vector for the kth class,
$\boldsymbol{\Sigma}_k$ = the covariance matrix for the kth class,
P_k = the *a priori* probability for the kth class,
L_k = the likelihood function for the kth class, and
$\mathbf{x}$ = the observation vector.

Ground areas of homogeneous landform and land-cover conditions were identified through a field study reported by Satterwhite and Ehlen (1980). Landform and land-cover data and maps from that

TABLE 1. LAND-COVER LEGEND FOR FIGURE 2

Map Symbol	Land-Cover Unit
10	Grass
12	Grass-*Flourensia cernua*
14	Grass-*Artemisia filifolia*
15	Grass-*Prosopis glandulosa*
16	Grass-*Parthenium incanum*
20	*Larrea tridentata*
21	*Larrea tridentata*-Grass
23	*Larrea tridentata-Prosopis glandulosa*-Grass
25	*Larrea tridentata-Flourensia cernua*
30	*Acacia constricta*-Grass
31	*Acacia constricta-Larrea tridentata*-Grass
40	*Flourensia cernua*-Grass
41	*Flourensia cernua-Larrea tridentata*
50	*Prosopis glandulosa-Atriplex canesens-Xanthocephalum Sarothrae*-Grass
51	*Prosopis glandulosa-Larrea tridentata*
52	*Prosopis glandulosa-Artemisia filifolia*-Grass
60	*Artemisia filifolia*-Grass
61	*Artemisia filifolia-Prosopis glandulosa*-Grass
70	*Juniperus monosperma-Quercus undulata*
90	Bare Rock
92	Urban and built-up areas

study formed the ground truth data base for our field definition and class identification in this study. The corresponding areas in the digital imagery provide spectral signatures for the classes of interest. The digital computations were performed using the classification programs developed by Rice *et al.*, (1978, 1980).

The study area was delineated on each of two unrectified Landsat images; number 2059-16590, dated 22 March 1975, and number 2221-16575, dated 31 August 1975. Two regions were identified within the study area for detailed evaluation: (1) the Meyer region in the eastern part and (2) the Dona Ana in the western part. The definition of training fields in the Landsat image for the classification process was highly selective and interactive. These were positioned within a land-cover mapping unit as determined by visual comparison with the ground truth data base and, where possible, contained 100 or more pixels.

Although the dates of the Landsat imagery used here and the dates of the field work do not coincide, changes in land-cover conditions between these two dates were very small and not identifiable from remotely sensed imagery. This assessment is based on the rather slow rate of plant establishment and growth in this semi-arid region and the fact that no large, recently disturbed areas were found during the field effort.

A class was created from each training field. Each class was composed of the collection of pixel intensity vectors (bands 4, 5, 6, and 7 of the Landsat scene) interior to the training field. The mean vector and covariance matrix were calculated to develop the spectral signature representative of a land-cover mapping unit in which the training field was placed. Class spectral signatures were first evaluated for uniformity. Those having a standard deviation less than 3 in all bands were considered representative of a homogeneous land-cover mapping unit. For all class spectral signatures, a pairwise Bhattacharyya distance (Kailath, 1967) between the signatures was computed. As a working rule a Bhattacharyya distance of 0.3 was taken as the value which separated similar classes (>0.3) from dissimilar classes (<0.3). In those cases in which separate training fields led to similar classes, the similar classes were combined into a single class. In other cases in which two separate training fields thought to contain the same material led to distinctly dissimilar classes, both classes were retained for the maximum likelihood classification process in order to clarify the situation. The classes created in each study region were only used to classify the region in which they were defined.

As a final step in the class selection process, a preliminary classification of the two regions was performed. The homogeneity of each spectral class was measured by the classification of the pixels in the training field belonging to the class. A decision

threshold of 70 percent of pixels correctly classified was required to conclude that the class represented a homogeneous land-cover unit. Several iterations of the class formation and the class selection process were required to derive an acceptable set of classes for each region.

CLASSIFICATION RESULTS OF THE MEYER REGION

Once class signatures were developed, the two study regions in the two Landsat images were classified. For brevity, only the results for the Meyer Region from the March image will be discussed in this section. Further detailed classification results are reported by Satterwhite (1982).

The Meyer region is 340 pixels wide and 360 lines long covering an area 27.2 by 28.8 km². The labeled polygons defining the training fields are shown in Plate 1. By convention, the false color composite image was created by setting the blue color to MSS band 4, green to MSS band 5, and red to MSS band 7. Through the iterative process described above, eight spectral classes were created that represented the 21 land-cover units in this region. Not all the land-cover units were characterized by discrete spectral classes. Some distinct land-cover classes that had been recognized in the field were not identifiable on the Landsat image because of their small size. Other land-cover units had similar signatures and were grouped into a single spectral class. The land-cover units selected for the supervised digital classification were *Scleropogon brevifolius-Hilaria mutica* (10C), *Sporobolus flexuosus-S. cryptandrus* (10D), *Bouteloua curtipendula-Parthenium incanum* (16), *Larrea tridentata* (20), *Larrea tridentata*-grassland (21), *Prosopis glandulosa-Atriplex canescens-Xanthocepthalum Sarothrae* (50), *Artemisia*

TABLE 2. SUMMARY OF CLASSES AND ASSOCIATED FIELDS FOR THE MEYER REGION.

Spectral Class	Color*	Training Field**
10C	Red	(10C-2), (10C-3), 21-7
10D	Green	(10D-2), (10D-3), 60-2
16	Gold	(16-3), 16-2, 20-3, 90-2
20	Blue	(21-7), 20-2, 21-1, 21-6
21	Buff	(21-4), 10C-2, 10C-3, 20-2, 21-1, 16-2, 16-3, 20-3, 21-6
50	Brown	(50-3), (50-4), 60-2, 50-5
60	Yellow	(60-3), 50-4, 60-2, 50-5
90	Purple	16-2, 16-3, 90-2

* The color represents the class in Plate 2.
** Fields listed have ≥10 percent of the pixels of the field classified into the spectral class shown.

The ( ) symbol indicates ≥70 percent of the pixels of the field classified into the spectral class shown. The (___) symbol represents ≥90 percent of the pixels of the field classified into the spectral class shown.

filifolia-grass (60), and bare rock (90). The maximum likelihood classification of the training fields is summarized in Table 2. Note that the pixels of some fields were classified to several classes representing different land-cover conditions. For example, field/class 16-2 had pixels classified in classes 16, 21, and 90.

Identification of these land-cover units provides at least a level 3 classification according to Anderson's system (Anderson *et al.*, 1976). Furthermore, the identification of the individual grasslands (10C) and (10D) provides a level 4 classification according to the Anderson system.

The color enhanced image of the classification of the March scene depicts the 8 spectral classes representing the 21 land-cover units (Plate 2). Visual
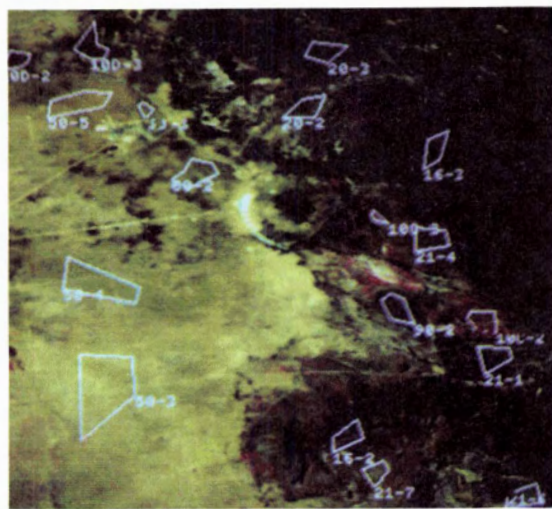

PLATE 1.   False color composite Landsat image; Meyer region, March scene. Labeled polygons represent training fields in selected land-cover units used in the digital classification process.

PLATE 2.   Color enhanced classified Landsat image; Meyer region, March scene. Numbered polygons correspond to those in Plate 1.

inspection of the image clearly shows that the outline of the level 3 shrub dominated communities is the same as that given in the ground truth image (Figure 2), and in some instances the level 4 grassland shrub communities also agree.

For example, the brown color on Plate 2 has similar distribution and configurations as the Number 50 mapping unit (level 3) on Figure 2. The green areas (10D) on Plate 2 closely approximate the *Sporobolus* grasslands on the basin areas of Figure 2.

Statistical confirmation was obtained by placing test fields interior to the land-cover units and ob-

serving the percent of correct classification, which was usually above 80 percent.

Because of the relationship between landform and land cover, the following detailed discussion of the study results is presented for each of the major landform units: Basin, alluvial fan and wash, and mountains/hills.

BASIN AREA RESULTS

In the basin area the land cover was comprised of grass, shrub, grass-shrub, and shrub-grass communities, dominated by *Prosopis glandulosa* or *Artemisia filifolia* shrubs or *Sporobolus flexuosus* and *S. cryptandrus* grasses. These species formed sev-

PLATE 3. False color composite Landsat image; Dona Ana region, March scene. Labeled polygons represent training fields in selected land-cover units used in the digital classification process.

PLATE 4. Color enhanced classified Landsat image; Dona Ana region, March scene. Numbered polygons correspond to those in Plate 3.

PLATE 5. False color composite Landsat image; Dona Ana region August scene. Labeled polygons represent training fields in selected land-cover units used in the digital classification process.
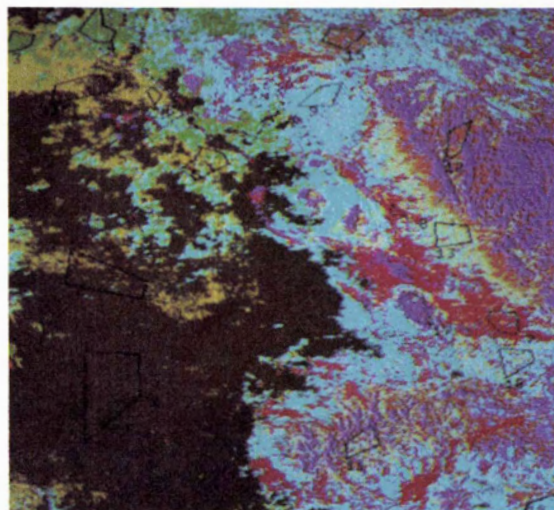

PLATE 6. Color enhanced classified Landsat image; Dona Ana region, August scene. Numbered polygons correspond to those in Plate 5.

eral land-cover units by their association with each other as either the dominant or subdominant species. The major land-cover unit is the *Prosopis glandulosa-Atriplex canescens-Xanthocephalum Sarothrae*-grass community (50). The smaller important land-cover units are *Sporobolus flexuosus-S. cryptandrus* grassland (10D) and *Artemisia filifolia-Sporobolus flexuosus* community (60).

Difficulty was encountered in separating some areas of the 60 and 10D land-cover units because of the grass cover within these land-cover units. The supervised classification also did not recognize other grass-shrub and shrub-grass units found in this region. The species forming these land-cover units were either the dominant or subdominant species in communities that occurred on similarly textured soils—either sands, sandy loams, or loamy sands. These communities were spectrally similar and were classified as the larger of land-cover units. For example, the *S. flexuosus* community (10D) was not differentiated from the *S. flexuosus-A. filifolia* (14) or *A filifolia-P glanduloas-S. flexuosus* (61) communities because of the dense grass cover in these land-cover units.

The major basin community, *Prosopis glandulosa-Atriplex canescens-Xanthocephalum Sarothrae*-grass (50), is a unique spectral class because of its moderate and uniformly distributed plant cover and large percentage of rather uniform soil conditions. Most of the spectral signature was from the sandy textured soils, with the vegetation providing a modifying affect.

ALLUVIAL FANS AND WASHES RESULTS

The land cover on the alluvial fans and washes was primarily shrub and shrub-grass communities with some grass and grass-shrub communities. The dominant plant species on the fan and some wash areas is *Larrea tridentata*, whereas *Flourensia cernua* shrubs and the grass species *S. brevifolius* and *H. mutica* dominate some sizable areas. *Prosopis glandulosa* is an associate species in some *Larrea tridentata* and *Flourensia cernua*-grass communities on the intermediate and lower alluvial fans.

Spectral classes 16, 20, 21, and 90 were located on the upper alluvial fans and limestone hills. The distribution of these land-cover units on the digitally classified image was often different from their distribution on the ground truth data base. This difference is a result of the large percentage of bare soil and rock in these landform units and the low percentage of vegetative cover.

Spectral class 21 corresponds to the intermediate and lower alluvial fans and to some portions of the wash landform. *Larrea tridentata* is the dominant species in these areas. The red toned areas on the color composite image (Plate 1) represents parts of some lower fans and washes where vegetative cover is more dense. Species in these areas include *Flour-*

ensia cernua and *Larrea tridentata* shrubs and the grasses *Hilaria mutica* and *Scleropogon brevifolius*.

Most wash and playa areas are similar to the *Scleropogon brevifolius-Hilaria mutica* grassland (10C). *Flourensia cernua*-grass (40) and grass-*Flourensia cernua* (12) units have spectral signatures similar to *Scleropogon brevifolius-Hilaria mutica* grassland (10C) and were classified accordingly. Some lower portions of the washes and playas had spectral signatures similar to that of the bare rock unit (90) and were confused with it.

MOUNTAINOUS AREAS

Land-cover units in the mountainous areas are characterized by two land-cover classes, *Bouteloua curtipendula-Parthenium incanum* (16) and bare rock (90). The rock outcrops were frequently confused with the classes 16, 20, and 21 on the upper alluvial fans which were covered with coarse textured particles derived from the limestone. These gravels on the upper fans and the high percentage of exposed bedrock in the mountains account for the spectral similarity of the upper fans and mountainous areas.

SEASONAL RESULTS

The phenological effects of vegetation on the classified Landsat images were evaluated by comparing the class mean signatures and the spatial distributions of the spectral classes in the March and August scenes for the Dona Ana region (Plates 3 and 5). Shrub communities dominated the land cover in the Dona Ana region: *Larrea tridentata* and *Prosopis glandulosa* with grass and grass-shrub communities. The forest community, *Juniperus monosperma-Quercus undulata* (70), and bare rock (90) occur at the highest elevations. The major land-cover units selected for the evaluation of seasonal difference were *Scleropogon brevifolius-Hilaria mutica* (10C), *Larrea tridentata* (20), *Larrea tridentata*-grassland (21), *Larrea tridentata-Prosopis glandulosa* (23), *Prosopis glandulosa-Atriplex canescens-Xanthocephalum Sarothrae* (50), *Juniperus monosperma-Quercus undulata* (70), and bare rock (90).

The labeled polygons defining the 18 training fields of the Dona Ana region for the March and the August scene are shown in Plates 4 and 6, respectively, with the legend for these plates presented in Table 3. Because the training fields for the two regions were positioned in the same land-cover units and covered the same geographical area in the two scenes, the differences between class signatures in the two scenes were attributed to temporal changes in the vegetative cover and plant growth characteristics. It is recognized that the observed differences may be due to illumination changes or atmospheric attenuation, but the attribution to temporal changes is the more convincing one for the following reasons.

Cool season species, which have maximum

TABLE 3. LAND-COVER CLASSES AND ASSOCIATED COLOR FOR THE DONA ANA REGION.

Land-Cover Unit	Land-Cover Class	Color
Scleropogon brevifolius-Hilaria mutica	10C	Red
Larrea tridentata	20	Blue
Larrea tridentata-grassland	21	Buff
Larrea tridentata-Prosopis glandulosa	23	Orange
Prosopis glandulosa-Atriplex canescens-Xanthocephalum Sarothrae	50	Brown
Juniperus monosperma-Quercus undulata	70	Green
Bare rock	90	Purple

growth during the early spring or late fall, and the warm season species, which have maximum growth during the summer and early fall, would have cover differences during these periods when compared with other times of the growth cycle. Depending on the vegetation's spectral characteristics and the percentage of ground covered, the vegetative cover would change the class signature in such a way that the seasonal differences between the class signatures would be associated with the periods of maximum vegetative growth. This association was in fact observed.

The August:March ratio of the two mean vectors for each class in the Dona Ana region (Table 4) show that land-cover units (20, 23, 50, and 90) had higher reflectance in the March scene than in the August scene. These land covers are comprised mostly of warm season species that achieve maximum growth and vegetative cover during the August-September period. In this regard, the warm season species in the March scene were devoid of leaves or were in a reduced leaf stage. This enables a greater percentage of the highly reflective soil surface to form the class signature.

On the other hand, communities comprised of cool season grasses, shrubs, and trees (10C and 70) had low reflectance in bands 4 and 5, but high re-

flectance in bands 6 and 7 for the March scene. The relation of low reflectance in the visible region and high reflectance in the infrared region indicates actively growing vegetation, with a high percentage of cover on the highly reflective soils. This condition was seen for class 21 in which the cool season grass cover increased in March, but decreased in the August scene when these grasses were dormant.

MAJOR LANDFORM UNITS

Major land-cover units in the Dona Ana region had the same general distribution on both classified images (Plates 4 and 6), but some differences were noted. These differences between scenes are summarized below by major landform units, using the March scene as the reference.

BASIN

- Reduction of the *Larrea tridentata-Prosopis glandulosa* community (23) but an increase in *L. tridentata*-grass (21).
- Increase of the *Juniperus monosperma-Quercus undulata* (70) (a misclassification of land cover) but a reduction in the *Larrea tridentata-Prosopis glandulosa* (23) and *Larrea tridentata*-grass (21) in the transition from the basin to the alluvial fans.
- Increase in the *Scleropogon brevifolius-Hilaria mutica* grassland (10C).

ALLUVIAL FANS

- Increase in bare rock (90) and decrease in *L. tridentata* (20) and *L. tridentata*-grass (21) on the alluvial fans of the mountains.
- Increase in *L. tridentata* (20) and decrease in *L. tridentata*-grass (21) on fans around some mountain areas.
- Increase in *Larrea tridentata* (20) but decrease in bare rock on the alluvial fans of some mountain areas.

MOUNTAINS/HILLS

- Decrease in *Juniperus monosperma-Quercus undulata* (70) and increase in *L. tridentata* (20).
- Decrease in bare rock (90) and increase in *L. tridentata* (20).
- Decrease in *Scleropogon brevifolius-Hilaria mutica* (10C) (a misclassification of land cover) and increase in *L. tridentata* (20).

TABLE 4. RATIO OF THE CLASS MEANS IN THE 4 LANDSAT BANDS FOR THE MARCH IMAGE TO THOSE OF THE AUGUST IMAGE

Class	Landsat Band*			
	4	5	6	7
	Ratio Values			
10C	0.89	0.80	1.30	1.60
20	0.93	0.92	0.90	0.95
21	0.83	0.80	0.93	1.04
23	0.94	0.99	0.92	0 97
50	0.90	0.95	0.91	0.97
70	1.05	1.17	0.97	0.98
90	0.81	0.81	0.88	0.97

* An August:March ratio of less than 1.00 indicates that the intensity was greater for the March scene signature than for the August scene signature.

Discussion

The level 3 land-cover classification achieved from these Landsat scenes was possible using prior knowledge of the relations between the land cover and the landform conditions. The larger land-cover units on the alluvial fans, basins, and mountain areas had spectral reflectance characteristics sufficiently different that they could be digitally separated and mapped on the Landsat image. For other land-cover units, their spectral reflectance characteristics were similar to the larger units and could not be separated. The confusion observed on the classified image could be resolved through an evaluation of the landform-land cover associations and by using the species phenological characteristics. General landform conditions are visually recognizable on the color composite Landsat image and were used in the image analysis process. Understanding the soil texture and soil depth conditions commonly associated with these landform units, i.e., coarse-textured shallow soils on upper alluvial fans and mountain areas, and fine-textured deep soil on the lower fans, playas, and basins, showed the "out of place" land-cover class on a landform unit, and point out the need for additional class evaluation. Although not done in the present study, confusion between land covers could be further reduced from the classified map by incorporating landform data derived from an elevation data base, such as that available from the National Cartographic Information Center (NCIC), into the image classification process.

The spectral signatures of some playas and the mountainous areas in the Meyer and Dona Ana regions were similar, which led to the classification of the playa as rock outcrops associated with mountainous areas. Left unresolved, the class map showing this error could lead to management practices that were reasonable for one condition but not for the other. The playa lake is a flat area with silty clay soils and the other area a rugged, rocky, mountainous region with little or no soil. Instances such as these necessitate the use of landform data in the image evaluation and analysis.

In the study regions, the intensity range was narrow in all the bands, amounting to 30 out of the 256 levels in bands 4 and 7 and 75 levels in bands 5 and 6. Compounding this, two land-cover units can have different spectra; but when integrated over the wavelengths assigned to a given band, they will have the same average intensity value. In such a case, the two objects would be combined into the same spectral class.

Visual comparison of the ground truth maps and the digital classified maps show differences in the spatial distribution of some land-cover units. Generally, these differences were between the land-cover units that occurred on the same major landform condition: basin, alluvial fans and washes, or mountains and dissected hills. The explanation for this involves the phytosociological differences, percent vegetative cover, similar soil conditions in these landform units, and seasonal effects.

The phytosociological difference found in the field data were not reflected in the class signatures associated with some land-cover units. For example, land-cover units *Sporobolus flexuosus-Artemisia filifolia* (14) and *Artemisia filifolia-S. flexuous* (60) had the same species compositions, but they varied by the dominants in the community. Both communities had the same spectral signature. Furthermore, a distinct signature was often not associated with the dominant species of a land-cover unit. The need for a distinct signature for each land-cover category is the reason that a level 4 land-cover classification, possible with field data, was not obtained from the digital data.

The similar spectral signatures for some communities apparently resulted from the dense grass cover. This was found in grass-shrub and shrub-grass communities where the shrub species lacked the reflectance contrast with the understory and soil background and the coverage to provide a discriminating signature. In these instances the more dense grass cover provided the major portion of the class signature (i.e., communities 14, 15, 60, and 61). Similarly, different communities with low vegetative cover on the same soil conditions were often confused because the soil's signature was not attenuated by the vegetative cover. This was found in the basin where some *P. glandulosa* communities (50) were confused with the sparsely vegetated *S. flexuosus* (10D) and *A. filifolia* (60) communities.

Different land-cover units that occurred on dissimilar land-form conditions could have similar spectral signatures caused by shadows, dense dormant plant material, debris, or surficial gravels, which caused confusion in the land-cover classification. Shadows in the mountain areas of the Dona Ana region were similar to the dense dormant vegetative cover in the playas and depression of the basin in both the March and August scenes. The dense dormant vegetative cover on the lower fans and in the basin depressions were also spectrally similar.

In some instances the surficial materials that mantled the upper fans and some intermediate fans with a layer of gravel-sized particles were often spectrally similar to the bedrock parent material.

Most soils in the Meyer and Dona Ana regions were highly reflective. Thus, when a large percentage of bare soil occurred in a land-cover unit, the soil's reflectance characteristics dominated the signature of the land cover. The reflectance from these soils is much greater than for green vegetative cover, e.g., *Prosopis glandulosa* in the visible region, and is slightly less in the infrared region. For gray-toned vegetation, e.g., *Artemisia filifolia,* the reflectance contrast between soil and vegetation in the visible range is still large, but it is less than that

for a green vegetation. In the infrared region, soil and A. *filifolia* reflectance contrast is quite small. Thus, changes in the vegetative cover that naturally occur over the growth cycles can change the reflectance contrast of the land surface and the land-cover class signature.

The data presented in Table 4 show these seasonal changes in the reflectance of the land-cover units, and different class signatures for the two scenes. The seasonal vegetative growth in some land-cover units, which is depicted by the red or reddish-colored areas in the March color composite image, is not distinguished by the same red color in the August scene. The reddish areas in the March scene indicate a dense vegetative cover, most probably cool season grasses. The comparison of the seasonal imagery shows the shrub-grass and grass-shrub land-cover units with a dense cover are represented by the red color. Some shrub and shrub-grass communities land cover were not apparent on either image, although the shrub species were fully leafed out and the warm season grasses were actively growing in the August scene. The reason for this was the low vegetative cover in these communities. The differences in the land-cover classification resulted from seasonal changes in the vegetative cover rather than from dramatic change in species composition. As the seasonal imagery illustrates (Plates 3 and 5), the seasonal differences in ground cover can vary substantially over the growth cycle of both the cool and warm season species.

CONCLUSIONS

Understanding the species' annual growth cycles and the relations of cover and soil reflectance, coupled with the knowledge of species-landform relations, soil-landform relations, and anticipated seasonal reflectance responses, can help in the interpretation of classified digital images. This interpretation is a nontrivial matter that must rely on ground truth information and certain other data for inferring plant-landform-soil relations. If properly used, this information could enable a level 3 or level 4 digital classification.

The significant finding from comparing classified seasonal images was rather consistent mapping of the major land-cover landform conditions. The spectral classes in each scene are indicative of uniform or closely related conditions. However, there was some confusion in the land-cover classification of the same geographical area on the seasonal imagery.

The factors affecting the class signatures were the seasonal variations in percentages of vegetative cover, dormant biomass, and bare soil/rock within the land-cover units. These changes resulted in some grass-shrub and shrub land-cover units being misclassified. Some areas were classified to one class in the March scene and as another in the August scene. The variations in class signature were explainable, in part, by seasonal vegetation growth characteristics.

As has been shown, the use of landform-cover relations can increase the level of classification of digital images. These relations facilitate the separation of spectrally similar but different plant communities by their landform associations. Using these relations with elevation data in an automated procedure would have the effect of adding new dimensions to the intensity vectors.

REFERENCES

Anderson, J. R., E. E. Hardy, J. T. Roach, and R. E. Witmer, 1976. *A Land Use and Land Cover Classification System for Use with Remote Sensor Data*, U.S. Geological Survey Professional Paper 964.

Fu, K. S., 1976. Pattern Recognition in Remote Sensing of Earth Resources, *IEEE Trans. on Geoscience Electronics, 14*, p. 60.

Fu, K. S., T. Landgrebe, and T. L. Phillips, 1969. Information processing of Remotely Sensed Agricultural Data, *Proceedings of the IEEE, 97*, p. 639.

Kailath, Thomas, 1967. The Divergence and Bhattacharyya Distance Measures in Signal Selection, *IEEE Trans. on Communication Technology, 15-1*, pp. 52-60.

Rice, W. C., J. S. Shipman, and R. J. Spieler, 1978. *Interactive Digital Image Processing Investigation*. U.S. Army Engineer Topographic Laboratories, Fort Belvoir, Va., Report ETL-0172.

———, 1980. *Interactive Digital Image Processing Investigation, Phase II*. U.S. Army Engineer Topographic Laboratories, Fort Belvoir, Va., Report ETL-0221.

Satterwhite, M. B., 1982. *Some Vegetation and Terrain Effects on Digital Classification of LANDSAT Imagery*, U.S. Army Engineer Topographic Laboratories, Fort Belvoir, Va., Report ETL-0292.

Satterwhite, Melvin B., and J. Ehlen, 1980. *Vegetation and Terrain Relationships in South-Central New Mexico and Western Texas*, U.S. Army Engineer Topographic Laboratories, Fort Belvoir, Va., Report ETL-0245.

Satterwhite, M. B., J. P. Henley, and M. Trieber, 1982. *Vegetative Cover Effects on Soil Spectral Reflectance*, U.S. Army Engineer Topographic Laboratories, Fort Belvoir, Va., Report ETL-0284.